

Single-Crystal Structure and Electron Density Distribution of Ammonia at 160 K on the Basis of X-ray Diffraction Data

Roland Boese,* Norbert Niederprüm, Dieter Bläser, and Andreas Maulitz

Institut für Anorganische Chemie, Universität-GH Essen, Universitätsstr. 3-5, 45117 Essen, Germany

Mikhael Yu. Antipin*

Institute of Organoelement Compounds, Russian Academy of Sciences, Vavilov St. 28, B-334, Moscow 117813, Russia

Paul R. Mallinson

Chemistry Department, University of Glasgow, Glasgow G12 0, U.K.

Received: February 17, 1997; In Final Form: April 17, 1997[®]

A single-crystal of ammonia, NH_3 , was grown in a thin-walled capillary at 178 K, and high-resolution X-ray diffraction data were obtained for this compound at 160 K in order to obtain information about electron density distribution. Conventional and multipole refinements and deformation electron density maps indicated small but significant N–H bond bending inside the NH_3 tetrahedron that is in agreement with *ab initio* quantum-chemical calculations and the VSEPR model. Topological analysis of the experimental charge density distribution in the ammonia molecule has been performed, and the data are compared with high-level quantum-chemical calculations. Some features of the intermolecular hydrogen bonds in the crystal are discussed.

Introduction

Ammonia has received much attention in the last years. Because of its simple structure, this molecule has been the subject of numerous calculations dealing with the questions of hybridization,¹ bond bending,^{1,2} lattice dynamics,³ and hydrogen bonding,^{4–7} including the structure of the ammonia dimer^{5,6} and oligomers.⁷ In a series of very recent publications^{8–11} the molecular geometry and other molecular and charge density properties of ammonia were calculated using various levels of the modern *ab initio* molecular orbital calculations^{8,9} or density functional theory.^{10,11}

Nevertheless, despite the interest in this small molecule, diffraction studies of the ammonia crystal are very rare. Earlier structural studies either were limited to the very low resolution and low accuracy of the X-ray data (photographic registration at 113 K, $\sin \theta/\lambda < 0.58 \text{ \AA}^{-1}$, see ref 12) or were done by the powder neutron diffraction of the deuterated samples (data at 77 K, $\sin \theta/\lambda < 0.46 \text{ \AA}^{-1}$, in ref 13; data at 2, 77, and 180 K with the maximum $\sin \theta/\lambda = 0.85 \text{ \AA}^{-1}$ in ref 14). In all these studies the cubic crystal structure of ammonia was confirmed (space group $P2_13$, $Z = 4$) with the special position for the N atom on a 3-fold axis (x, x, x) and one H atom in the general position (x, y, z).

On the other hand, modern single-crystal X-ray diffraction analysis allows one to reconstruct an electron (or charge) density distribution $\rho(\mathbf{r})$ in molecules and crystals^{15,16} with a high accuracy and thus to give a new experimental confirmation of some important and widely used concepts in structural chemistry, related directly with the electronic nature of the chemical bond. Among these concepts we should note the bond-bending concept¹⁷ and the VSEPR model,¹⁸ based directly on analysis of features of the observable $\rho(\mathbf{r})$ function.

A modern approach in analysis of $\rho(\mathbf{r})$ in crystals, experimentally reconstructed from the high-resolution X-ray diffraction

data, consists in an analytical presentation of the continuous electron density distribution of the unit cell as a sum over pseudoatom densities centered at nuclear sites. One of the more widely used approximations is the Hansen and Coppens multipole model for presentation electron density of the aspherical atom in the crystal as a series of the Slater-type radial functions modulated by the real spherical harmonics.¹⁹ This model is sufficiently flexible to describe asphericity of the atomic electron density in crystals caused by the chemical bonding and interatomic interactions. Detailed descriptions of the Hansen and Coppens approach and other multipole models and their application in the charge density analysis are given elsewhere.^{20,21}

Multipole presentation of $\rho(\mathbf{r})$ allows one to perform a rigorous description of the chemical bonds and atomic interactions through the study of topology of the total electron density of the molecular system following Bader's quantum theory of atoms in molecules.²² In accord with this theory, important topological characteristics of $\rho(\mathbf{r})$ are summarized by the properties of its critical points \mathbf{r}_c , where $\nabla\rho(\mathbf{r}) = 0$. The number and signs of the principal curvatures of $\rho(\mathbf{r})$ at \mathbf{r}_c define two integer numbers (ω, σ), named rank and signature of the critical point, respectively. The rank ω is the number of nonvanishing eigenvalues of the Hessian matrix of $\rho(\mathbf{r})$ at \mathbf{r}_c , and the signature σ is the algebraic sum of signs of the principal curvatures (eigenvalues) of $\rho(\mathbf{r})$ at a critical point. From the chemical point of view the more important are (3, –1) critical points, or saddle points of the electron density, that define a bonding interaction between two atoms in a molecular system. Two atoms are said to be involved in a bonding interaction if there is a line (bond path) connecting their nuclei along which the electron density has a maximum with respect to any lateral displacements. The electron density attains its minimum value along a bond path at the position of the bond critical point. So, in the bond (3, –1) critical point the curvature of $\rho(\mathbf{r})$ in the bond direction is positive, and it is negative in the two other directions. In

[®] Abstract published in *Advance ACS Abstracts*, June 1, 1997.

TABLE 1: Results of the Ammonia Crystal Structure Refinement^a

	model						
	N(180 K)	N(2 K)	X1	X2	X3	X4	M
Refinement							
<i>N</i> (refl)			344	129	182	310	334
<i>N</i> (par)			9	9	4	5	26
refl/par			38.2	14.3	45.5	62	12.8
<i>R</i> (%)	6.17	2.24	1.87	0.86	3.15	3.42	1.19
<i>R</i> _w (%)			1.60	0.88	2.51	2.76	0.95
GOF			1.69	1.87	0.91	3.78	0.91
ext corr	no	no	yes	yes	no	yes	yes
Atomic Coordinates							
<i>x</i> (N)	0.2107(7)	0.2109(3)	0.21021(3)	0.21020(4)	0.21050(6)	0.21031(8)	0.2103(1)
<i>x</i> (H)	0.3689(6)	0.3750(3)	0.3458(6)	0.3456(7)	0.3740	0.3738	0.3722
<i>y</i> (H)	0.2671(6)	0.2712(4)	0.2519(8)	0.2563(9)	0.2608	0.2606	0.2627
<i>z</i> (H)	0.1159(7)	0.1129(3)	0.1294(6)	0.1297(9)	0.1131	0.1129	0.1113
Displacement Parameters							
<i>U</i> ₁₁ (N)	0.0384(8)	0.0101(4)	0.03688(8)	0.03671(14)	0.0358(2)	0.0365(2)	0.0372(2)
<i>U</i> ₁₂ (N)	−0.0014(7)	−0.0005(4)	−0.00061(6)	−0.00058(7)	−0.0011(1)	−0.0010(1)	−0.0009(1)
<i>U</i> (H)	0.064(2)	0.0101(9)	0.0528(8)	0.0520(9)	0.0528	0.0528	0.0530
Molecular Geometry							
N–N (Å)	0.989(5)	1.012(2)	0.838(3)	0.842(4)	1.010	1.010	1.010
H–H–H (deg)	107.8(4)	107.5(2)	109.0(2)	108.1(3)	109.0	109.0	109.0

^a Detailed description of models is given in the text. In the high-order models X3 and X4 only reflections with $|F| > 6.0\sigma(F)$ were used; the weight scheme in the X1–X4 refinements was $w^{-1} = \sigma^2(F)$, and in the refinement X4 a Seiler and Dunitz³² parameter, $B = 6.0$, was taken.

general, the bond path should not be a straight line, and namely, its deviation from that line defines a bond bending—important characteristic of the chemical bond—in terms of topological properties of the electron density distribution $\rho(\mathbf{r})$.

Another important topological characteristic of $\rho(\mathbf{r})$ is its Laplacian $\nabla^2\rho(\mathbf{r})$ —the sum of three curvatures of the total density. The negative values of Laplacian indicate those regions of the molecular space where a local charge concentration takes place, and corresponding Laplacian maps were found to be very useful in the analysis of the charge density and chemical bonds in addition to the conventional deformation electron density (DED) maps. It is important that Laplacian is calculated directly from $\rho(\mathbf{r})$, so it is not a model-dependent difference function as is DED (which is the difference between the total electron density and the density of the hypothetical “promolecule”, see refs 15 and 16 for details). Therefore analysis of the Laplacian maps may give additional independent information about electron density characteristics and chemical bonding in molecules and crystals.^{20–23}

Nevertheless, despite an obvious attractiveness of the multiple presentation of $\rho(\mathbf{r})$ and its topological analysis, there is a relatively small number of publications (see, for example, refs 24–30) where similar study of the experimental electron density distribution has been done for crystals of small and simplest molecules. In the present paper we report the X-ray diffraction investigation of the molecular and crystal structure and the electron density distribution in the single crystal of ammonia, NH₃, including topological analysis of the experimental and theoretical (calculations at the MP2/6-311G(3d) level) charge density in this small molecule.

Experimental Section and Refinement

In order to obtain a single crystal of ammonia, a thin-walled capillary (diameter 0.3 mm) was filled with condensed dried ammonia, sealed, and transferred to a diffractometer with a low-temperature device. A single crystal was grown directly on the diffractometer at 178 K using a miniature zone-melting technique producing a molten zone with a focused infrared light.³¹ After many attempts it was possible to grow a single crystal of high quality. Cooling down the sample below 160 K caused a

broadening of the reflection profiles; therefore the cell dimensions and X-ray diffraction experiment were carried out at 160 ± 0.5 K with a Nicolet R3m/V four-circle diffractometer using Mo K α radiation ($\lambda = 0.71069$ Å) and graphite monochromator. Cell dimensions and orientation matrix were determined at 160 K using 25 centered reflections in the interval $0.18 < \sin \theta/\lambda < 0.30$ Å^{−1}. Crystals of ammonia are cubic, space group *P*2₁3, at 160 K: $a = 5.1305(8)$ Å, $Z = 4$, $V = 135.05(8)$ Å³, $F(000) = 40$, $\mu = 0.06$ mm^{−1}, $d_{\text{calc}} = 0.838$ g cm^{−3}.

In the full sphere of the reciprocal space in the 2θ -interval 2.0 – 89.5° ($\sin \theta/\lambda < 0.99$ Å^{−1}), and using a Wickoff scan technique, a total number of 3683 reflections were collected, and 344 unique observable ones ($R_{\text{int}} = 0.021$, volume correction was applied taking into account a cylinder shape of the crystal) with $|F_o| > 4\sigma(F_o)$ were used in further refinements and calculations.

Starting from the Hewat and Riekel model of the ammonia crystal¹⁴ based on neutron powder diffraction data at 180 K (model N) and using the SHELXTL program package, the refinement of our single-crystal data with nine independent parameters including isotropic extinction correction converged very well ($R = 0.0187$, $R_w = 0.0160$, GOF = 1.69, model X1). When only low-angle data were included in the refinement because of relative weakness of the high-order intensities (129 reflections with $\sin \theta/\lambda < 0.70$ Å^{−1}), the residuals decreased much more significantly to $R = 0.0086$, $R_w = 0.0088$, GOF = 1.87 (model X2). Different models of the ammonia crystal structure are compared in Table 1.

In order to get information about electron density distribution in the ammonia molecule in crystal, corresponding DED maps were calculated using the standard “X–X” method^{15,16} in the plane of the N–H bond and 3-fold crystal axis, where a nitrogen atom electron lone pair (Lp) is assumed to be localized near the N atom in accord with VSEPR model.¹⁸ High-order ($\sin \theta/\lambda > 0.70$ Å^{−1}, 182 reflections with $|F| > 6\sigma$, model X3) and quasi-high-order refinement with the Dunitz and Seiler weight scheme³² at $B = 6.0$ (model X4) were used for calculating electron density of the “promolecule” in the evaluation of DED maps. In both calculations DED maps were similar in most details, and one of the maps (corresponding with the X4 model)

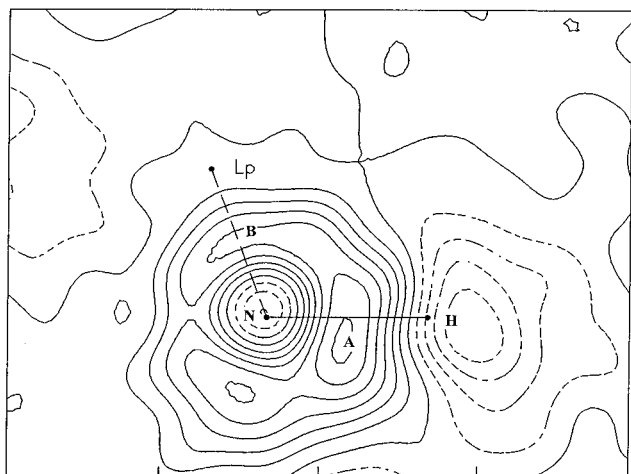


Figure 1. Dynamic DED map in the ammonia molecule ("X-X" method, isolines are drawn through $0.05 \text{ e}/\text{\AA}^3$, negative contours are dashed) in the plane of the N-H bond and 3-fold crystal axis, coincident with the direction of the nitrogen atom lone pair (Lp). The distance N-Lp is 1.0 \AA .

is presented in Figure 1. Hydrogen atom position in these refinements was fixed at 1.010 \AA on the prolongation of the N-H bond vector, and its isotropic displacement parameter (taken from the X1 model) was fixed too. It is interesting to note that in the high-order models the position of the N atom was slightly shifted to the expected direction, namely, away from the Lp position and closer to the H_3 plane, because the higher the $(\sin \theta/\lambda)_{\min}$ cutoff, the smaller the Lp contribution in the X-ray scattering. Comparison of atomic coordinates of different models shows that they are very close to those obtained in the neutron diffraction study, including H atom position after elongation of the N-H bond distance.

More detailed information about charge density distribution in ammonia including important quantitative characteristics of this distribution and its topological features was obtained using a multipole refinement and XD package program.³³ Results of this refinement (model M) are also included in Table 1. Taking into account crystal symmetry constraints and multipole expansion up to the hexadecapole level ($l = 4$) for N atoms and dipole level ($l = 1$) for H atoms, only 26 independent parameters were refined in this model, including nine multipole parameters for the N atom ($P_{\text{val}}, P_{10}, P_{20}, P_{30}, P_{33+}, P_{33-}, P_{40}, P_{43+}, P_{43-}$) and four parameters for the H atom ($P_{\text{val}}, P_{10}, P_{11+}, P_{11-}$). In addition, the k and k' parameters for the N atom (valence shell contraction-expansion adjustable parameters in the multipole model¹⁹), scale factor, and isotropic extinction correction were refined too. For the H atom the k value was fixed at 1.20; its coordinates and isotropic displacement parameter were taken from the conventional refinement (model X1) after elongating the N-H bond and were fixed too. Multipole model resulted in significant decreasing of residuals: $R = 0.0119$, $R_w = 0.0095$, and $\text{GOF} = 0.91$.

After this refinement a model static DED map in the same plane as in Figure 1 was evaluated (Figure 2), and some topological properties of the charge density in ammonia in the N-H bond were calculated including bond critical point position, Laplacian of $\rho(\mathbf{r})$, bond path, and bond ellipticity. Some of these data are summarized in Table 2 together with similar results of *ab initio* calculations. Theoretical calculation of the topological characteristics of $\rho(\mathbf{r})$ in ammonia has been performed for optimized molecular geometry at the MP2/6-311G(3d) level using Bader's "atom in molecule" approach.

Results and Discussion

Molecular Geometry. Present X-ray data showed the H-N-H angle in ammonia to be $109.0(2)^\circ$ and N-H bond length to be $0.838(3) \text{ \AA}$ that is quite normal taking into account that X-ray data usually give shorter X-H bond lengths. Bond angle H-N-H is close to the tetrahedral one and corresponds to sp^3 hybridization of the nitrogen atom. We may compare this angle with the values of 107.2° and 106.7° in the gas-phase studies of ammonia.^{34,35} Neutron powder diffraction data at 180 and 2 K gave bond angles at the nitrogen atom equal to $107.8(4)^\circ$ and $107.5(2)^\circ$ (see ref 14).

On the other hand, numerous modern quantum-chemical calculations of the molecular properties of ammonia including its geometry (see, for example, refs 5, 8, 10, and 11) result in rather differing values for the H-N-H angle, varying in the interval $104.2\text{--}108.3^\circ$ depending on the method of calculation or the basis set. Thus, in the very thorough *ab initio* study of ammonia,⁸ an influence of the atomic basis set on calculated molecular properties was systematically analyzed, and it was found that the value of the bond angle at the N atom varies in the interval $107.1\text{--}108.3^\circ$, almost covering a rather narrow interval of the experimental values. Different density functional theory (DFT) approaches¹¹ with various exchange and correlation functionals resulted in the H-N-H angle of $105.0\text{--}107.5^\circ$. In accord with ref 5, the best estimated Hartree-Fock-based theoretical parameters for the NH_3 geometry are $1.021 \pm 0.007 \text{ \AA}$ and $105.5 \pm 1.0^\circ$, respectively.

Our MP2/6-311G(3d) calculation resulted in a rather small H-N-H angle, 103.9° . Probably, this basis set is not able to describe correctly the nitrogen atom lone pair. Using the MP2/6-311+G(3d) basis set has lead to an increase of the H-N-H angle to 105.1° , and more sophisticated optimizations (CCSD/cc-pVTZ and CCSD/AUG-cc-pVTZ) resulted in the values of this angle of 106.0° and 106.6° , respectively. In the very recent calculation by Wiberg³⁶ with the more balanced basis set MP2/6-311G(2df, 2pd), the H-N-H bond angle was found to be 107.1° , which is still less than the experimental value in the crystal.

Analysis of the presented data shows that probably it is impossible now to make definite conclusions about changes of the molecular geometry of ammonia in a free state and in the crystal. Nevertheless, we may note that in most modern *ab initio* calculations the bond angle at the N atom is $1\text{--}2^\circ$ smaller than in the crystal. This is may be a result of the hydrogen bonding in solid ammonia. We should note, therefore, that recent DFT calculation⁵ of the ammonia H-bonded dimer showed an increase of the H-N-H angle in the dimer in comparison with that in a free molecule.

Bond Bending. None of the experimental or calculated H-N-H bond angles in ammonia corresponds to the ideal value of 109.5° for sp^3 hybridization of the nitrogen atom. In accord with refs 1 and 2, this may be interpreted in two ways. First, a decreasing of the bond angle from the ideal "tetrahedral" value may be caused by repulsion between the nitrogen lone pair and N-H bond electrons (in accord with the VSEPR model¹⁸). On the other hand, assuming p hybridization for N-H bonds, one might explain the observed angle due to repulsion between hydrogen atoms. This explanation is very attractive because one might expect that the lone pair electrons would prefer a low-energy s orbital. As a result, N-H bond bending should be observed in ammonia due to both of these effects.

First indication about bending of bonds in small acyclic molecules such as water, ammonia, and others belongs to Hirshfeld,³⁷ who made this conclusion on the basis of geometrical distortions in a series of molecules of the RXR' type,

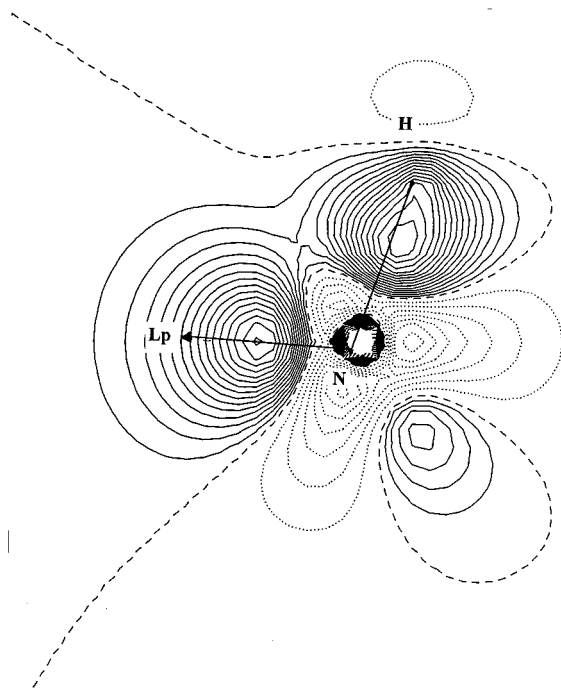


Figure 2. Static multipole DED map in ammonia in the same section as in Figure 1. Isolines are drawn through $0.05 \text{ e}/\text{\AA}^3$.

such as dimethyl ether, dimethyl sulfide, acetoxime, and some others. Bond bending for ammonia was proven later in ref 1 by the calculation of the bond path angles and their comparison with the conventional bond angles between the internuclear lines. It was established that bond angles in the ammonia molecule equal to 107.2° (6-31G* basis set), 107.5° (6-31G**), and 108.8° (6-31++G**) are systematically larger than corresponding bond path angles of 103.9° , 104.5° , and 106.3° , respectively. In the more recent calculation³⁶ using MP2/6-311G(2df,2pd) basis set, the corresponding bond angles and bond path angles were found to be 107.1° and 105.5° . So, N–H bonds in ammonia are bent inward in the NH_3 tetrahedron in accord with theoretical calculations. Unfortunately, no bond path analysis has been done for this molecule in the cited calculations.

We found in the present work that N–H bond bending in ammonia is evidenced directly in the experimental X-ray diffraction data in the dynamic (“X–X” method, Figure 1) and static (multipole model, Figure 2) DED maps that were calculated in the plane of the N–H bond and 3-fold crystal axis. The line N–Lp in these figures (1.0 \AA length) corresponds to the direction of the nitrogen atom electron lone pair.

In Figure 1 the height of the DED maximum (A) in the N–H bond is equal to 0.30 \AA^{-3} , and it is shifted from the N–H bond line by approximately 0.15 \AA away from the probable position of the nitrogen atom lone pair (B), i.e. inside the NH_3 tetrahedron. The nitrogen atom lone pair maximum (B) is not well resolved and rather diffuse. These features of the “X–X” maps manifest well in all models of the “high-order” refinements. In the static multipole DED map (Figure 2) the heights of maxima in the N–H bond and Lp area are much larger, resolution between these peaks is better, and main features of this map are very similar to those in Figure 1. The same N–H bond bending is observed in the multipole map, and the corresponding DED maximum in N–H bond is shifted from the bond line by approximately 0.08 \AA away from the Lp peak. So, N–H bond bending in the ammonia molecule has received direct experimental confirmation.

Hydrogen Bonding. As with water, one of the most important properties of ammonia is its ability to form hydrogen

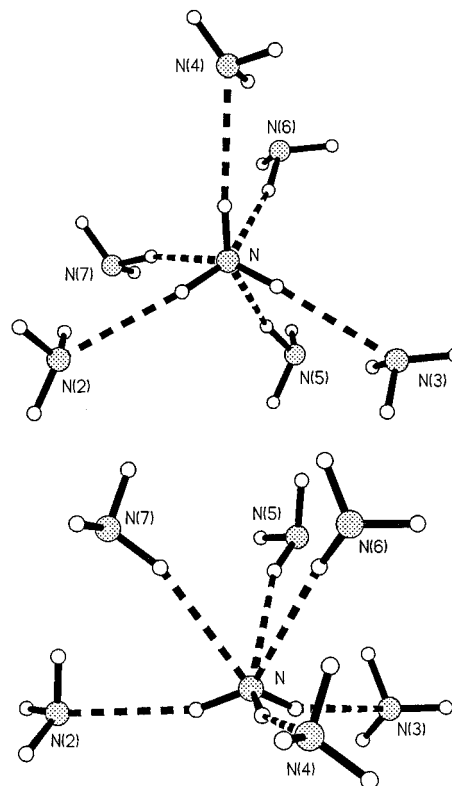


Figure 3. Hydrogen bond scheme of the reference NH_3 molecule in the crystal in two projections.

bonds. A study of these bonds in solid NH_3 is the subject of many publications, including very recent ones.^{5,6} In accord with earlier crystallographic data^{12–14} and the present work, in solid ammonia each NH_3 molecule acts simultaneously as a triple H-bond donor and triple H-bond acceptor. The geometry parameters of all of these six hydrogen bonds are similar because of crystal symmetry ($\text{N}\cdots\text{N}$, 3.378 \AA , $\text{H}\cdots\text{N}$, 2.40 \AA at the N–H distance 1.010 \AA and the N–H \cdots N angle 161.0°). The hydrogen bond scheme of the reference ammonia molecule in the crystal is presented in two projections in Figure 3. Three neighboring nitrogens (N(2), N(3), N(4)) are hydrogen acceptors from the central N atom, and the latter atom deviates from their plane by 0.468 \AA . The distance from the N atom to the plane of the three other N(5,6,7) atoms—hydrogen donors to N atom—is equal to 2.494 \AA .

Important characteristics of hydrogen bonding in the ammonia crystal were obtained from DED maps. Figure 4 shows DED section (“X–X” method) in the plane containing the central N atom and N(7)–H bond of the neighboring H-donor molecule. The N(6) atom, one of its hydrogens, and one of the H atoms of the central molecule are lying close to this plane (deviations from the plane are equal to -0.18 , 0.09 , and -0.11 \AA). This map is very similar to the figure in ref 7, where an *ab initio* calculation of the electron density distribution in solid ammonia has been carried out using 16-atom cluster surrounded by point charges as a model. It is clear from Figure 4 that there are areas of the negative DED outside hydrogens in the direction of hydrogen bonds. This may indicate an essentially electrostatic nature of this bond. Positive DED of the central N-atom lone pair is not clearly seen in this section because its maximum lies between the two $\text{N}\cdots\text{H}$ bonds and above the plane of the figure.

Additional information about H-bonding in ammonia follows from Figure 5 where two DED sections in the planes normal to the 3-fold axis pass through the nitrogen atom lone pair region at the distances 0.20 and 0.40 \AA from the nuclei. Small shifts

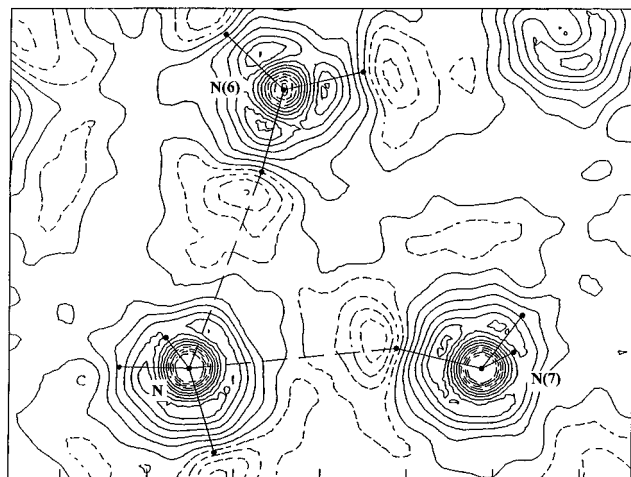


Figure 4. DED section ("X-X" method) in the crystal of ammonia showing the hydrogen bond formation in the plane of the reference N atom of the N(7)-H bond of the neighboring molecule. Isolines are drawn through $0.05 \text{ e}/\text{\AA}^3$.

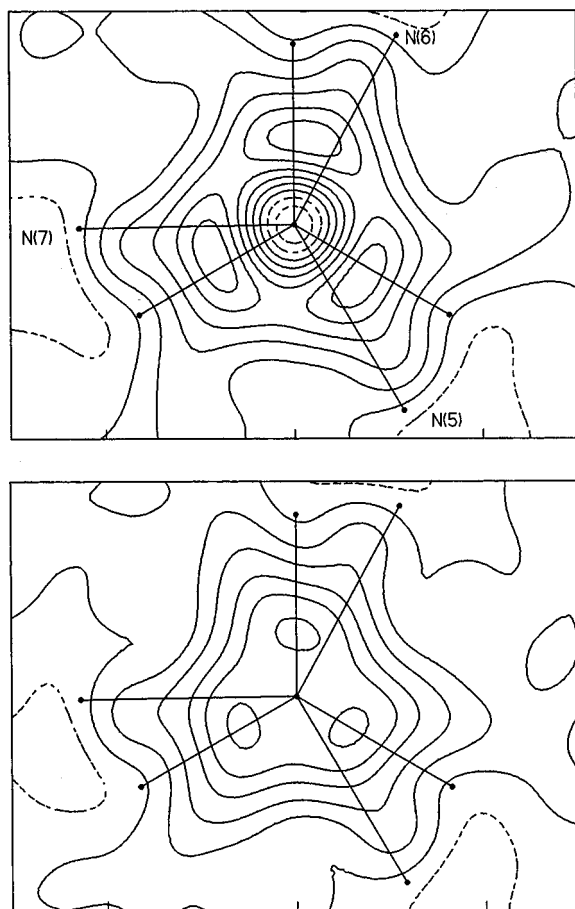


Figure 5. DED sections ("X-X" method, isolines as in Figure 1) of the ammonia molecule in the planes normal to the 3-fold axis and passing through the nitrogen atom lone pair at the distances 0.20 Å (top) and 0.40 Å (bottom) from the nuclei.

of the DED maxima of the nitrogen lone pair to the $\text{N}\cdots\text{N}(5,6,7)$ projection lines are observed, probably indicating some polarization of the lone pair electron density. This result indicates that the charge distribution in the NH_3 molecule in the crystal is determined both by the internal molecular geometry and, at least in part, by the spatial arrangement of the surrounding H-bond donors, which agrees with the theoretical data.⁷

Topology of the Charge Density. Some topological characteristics of the charge density distribution in the ammonia

TABLE 2: Topological Characteristics of the N-H bond and Some Molecular Properties of Ammonia in the Crystal

	X-ray experiment (multipole model)	ab initio calculations	
		MP2/6-311G(3d)	DFT methods ^a
$\rho(\mathbf{r}), \text{e}/\text{\AA}^3$	2.14(4)	2.18	2.21–2.30
$-\nabla^2\rho(\mathbf{r}), \text{e}/\text{\AA}^5$	28.9(12)	33.93	35.3–38.4
ellipticity	0.03	0.03	
$R(\text{N-H}), \text{\AA}$	1.010	1.017	1.004–1.028
$d(\text{N-cp})^b$	0.775	0.759	
$d(\text{cp-H})$	0.245	0.259	0.242–0.251
$\Delta, \text{\AA}$	0.010		
H-N-H bond			
angle (deg) ^d	109.0	103.9	105.0–107.5
bond path angle	107.5	101.5	
$\delta = 1.5^\circ$		$\delta = 2.4^\circ$	
dipole moment, D	1.50(6)		1.477–1.625 ^e

^a Theoretical calculations.¹¹ ^b d , distance from the atom nucleus to (3, -1) bond critical point (cp). ^c Δ , distance from the bond line to the bond critical point. ^d Experimental geometry in the gas phase: 1.012 Å and 106.7° (see ref 35). ^e Experimental value in the gas phase 1.47 D (see ref 35).

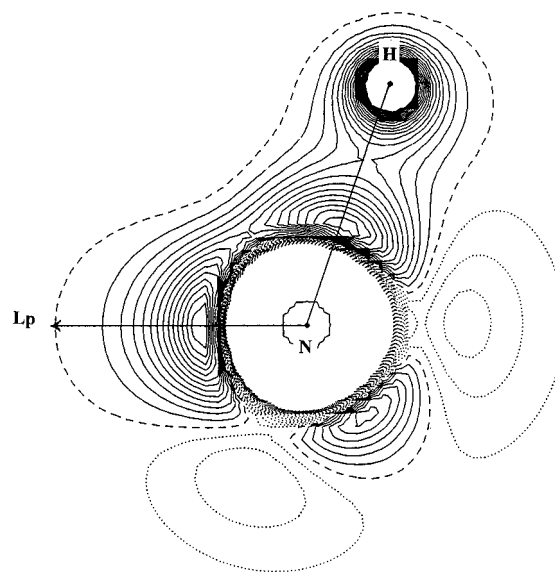


Figure 6. Laplacian map ($-\nabla^2\rho$) of the ammonia molecule in the same section as in Figures 1 and 2. Contours are given in the logarithmic scale.

molecule in crystal were calculated using the XDPROP option of the XD package program.³³ Corresponding results are presented in Table 2 and Figure 6. Results of our MP2/6-311G(3d) calculation of similar characteristics of ammonia, as well as some recent results of the DFT calculations,¹¹ are presented in the same table for comparison. We should note that despite numerous quantum calculations of ammonia (see above), a topological analysis of the charge density in this molecule has been performed only in ref 11 (some data are presented also in ref 9).

Laplacian map of ammonia (Figure 6) in the same section as in Figures 1 and 2 demonstrates clearly the concentration of its negative values in the N-H bond and nitrogen atom lone pair, thus confirming main features of the corresponding DED maps. Because Laplacian is not a difference quantity as is DED function, a similarity between these two maps may be an additional argument for the validity of our results.

As might be seen from Table 2, absolute values of the total electron density and its Laplacian in ammonia, as well as N-H bond ellipticity, calculated with the multipole model based on X-ray data and by *ab initio* calculations, are very similar. Bond critical point (3, -1) was found in the N-H bond. In accord

with electronegativities of atoms, this point is shifted closer to the H atom, which is in agreement with the theoretical calculations. In addition, multipole data resulted in the shift of the (3,−1) bond critical point from the N–H bond line by 0.010 Å inside the NH₃ tetrahedron thus indicating the bending of this bond, even though this shift is relatively small. It should be noted that calculated bond path angle in ammonia is smaller than the ‘valence’ bond angle. Similar result was noted in the theoretical calculation.¹

The dipole moment of ammonia in the crystal in accord with X-ray data was found to be 1.50(6) D, very close to the experimental value of 1.47 D in the gas phase,³⁵ and is in the interval of the theoretical values 1.477–1.625 D (Table 2). As was noted in ref 38, molecular dipole moments in crystals estimated from X-ray diffraction data are usually a little larger than those in the gas phase, but in general, X-ray multipole data result in very reasonable values of the molecular dipole moments, which was proven in the present paper for the ammonia molecule too.

Conclusion

Accurate X-ray diffraction study of the electron density distribution in the crystal of ammonia revealed N–H bond bending inside the NH₃ tetrahedron away from the position of the electron lone pair of the nitrogen atom. This result was evident not only in the DED maps (dynamic and static) but also in the topological analysis of the electron density distribution in the framework of Bader’s approach. Important characteristics of the charge density in N–H bond (total density, its Laplacian, bond ellipticity, bond critical point position) estimated from X-ray data on the basis of the multipole model were found to be in rather good agreement with results of quantum-chemical calculations. Together with some other examples of the bond bending in small acyclic and nonstrained organic molecules having atoms with lone pairs,^{39,40} our present results for ammonia allow one to suggest that the straight bonds indicated by “lines” between atoms might be more the exception than the rule.

Acknowledgment. M.Yu.A. is grateful to the Deutsche Forschungsgemeinschaft and R.B. acknowledges the Fonds der Chemischen Industrie for financial support.

References and Notes

- (1) Wiberg, K. B.; Mursko, M. A. *J. Mol. Struct.* **1988**, *164*, 355–365.
- (2) Politzer, P.; Abrahamsén, L.; Sjöberg, P.; Laurence, P. R. *Chem. Phys. Lett.* **1983**, *102*, 74–78.
- (3) Righini, R.; Klein, M. L. *J. Chem. Phys.* **1978**, *68*, 5553–5557.
- (4) Brink, G.; Glasser, L. *J. Mol. Struct.* **1987**, *160*, 357–364.
- (5) Novoa, J. J.; Sosa, C. *J. Phys. Chem.* **1995**, *99*, 15837–15845.
- (6) Platts, J. A.; Laidig, K. F. *J. Phys. Chem.* **1995**, *99*, 6487–6492.
- (7) Taurian, O. E.; Lunell, S. *J. Phys. Chem.* **1987**, *91*, 2249–2253.
- (8) Suter, H. U.; Ha, T. K. *J. Mol. Struct. (THEOCHEM)* **1993**, *102*, 151–162.
- (9) Aray, Y.; Casilimas, J. C.; Murgich, J. *J. Phys. Chem.* **1996**, *100*, 5291–5298.
- (10) Finley, J. W.; Stephens, P. J. *J. Mol. Struct. (THEOCHEM)* **1995**, *357*, 225–235.
- (11) Wang, J.; Johnson, B. G.; Boyd, R. J.; Eriksson, L. A. *J. Phys. Chem.* **1996**, *100*, 6317–6324.
- (12) Olovsson, J.; Templeton, D. H. *Acta Crystallogr.* **1959**, *12*, 832–836.
- (13) Reed, J. W.; Harris, P. M. *J. Chem. Phys.* **1961**, *35*, 1730–1737.
- (14) Hewat, A. W.; Riekel, C. *Acta Crystallogr. Ser. A* **1979**, *A35*, 569–571.
- (15) Coppens, P. *Annu. Rev. Phys. Chem.* **1992**, *43*, 663–692.
- (16) *The Application of Charge Density Research to Chemistry and Drug Design*; Jeffrey, G. A., Piniela, J. F., Eds.; NATO ASI Series; Plenum Press: New York, 1991; Vol. 250, 409 pp.
- (17) Coulson, C. A. *Valence*; Oxford University Press: London, 1952.
- (18) Gillespie, R. J.; Hargittai, I. *The VSEPR Model of Molecular Geometry*; Allyn and Bacon: Boston, 1991; Prentice Hall International: London, 1991.
- (19) Hansen, N. K.; Coppens, P. *Acta Crystallogr. Ser. A* **1978**, *34*, 909–921.
- (20) Stewart, R. F. In *The Application of Charge Density Research to Chemistry and Drug Design*; Jeffrey, G. A., Piniela, J. F., Eds.; NATO ASI Series, Plenum Press: New York, 1991; Vol. 250, pp 63–101.
- (21) Lecomte, C. *Ibid.* pp 121–153.
- (22) Bader, R. F. W. *Atoms in Molecules: A Quantum Theory*; Oxford University Press: Oxford, U.K., 1991.
- (23) Kraka, E.; Cremer, D. In *Theoretical Models of Chemical Bonding, Part 2. The Concept of the Chemical Bond*; Maksic, Z. B., Ed.; Springer-Verlag: Berlin-Heidelberg, 1990; 453 pp.
- (24) Howard, S. T.; Hursthouse, M. B.; Lehmann, C. W. *Acta Crystallogr. Ser. B* **1995**, *51*, 328.
- (25) Gatti, C.; Bianchi, R.; Destro, R.; Merari, F. *J. Mol. Struct. (THEOCHEM)* **1992**, *255*, 409–433.
- (26) Destro, R.; Merari, F. *Acta Crystallogr. Ser. B* **1995**, *51*, 59.
- (27) Koritsanzky, T.; Buschmann, J.; Luger, P. *J. Phys. Chem.* **1996**, *100*, 10547–10553.
- (28) Yufit, D. S.; Mallinson, P. R.; Muir, K. W.; Kozhushkov, S. I.; DeMeijere, A. *Acta Crystallogr. Ser. B* **1996**, *52*, 668–676.
- (29) Flensburg, C.; Larsen, S.; Stewart, R. F. *J. Phys. Chem.* **1995**, *99*, 10130–10141.
- (30) Roversi, P.; Barzaghi, M.; Merati, F.; Destro, R. *Can. J. Chem.* **1996**, *74*, 1145–1161.
- (31) Brodalla, D.; Mootz, D.; Boese, R.; Ojwald, W. *J. Appl. Crystallogr.* **1985**, *18*, 316.
- (32) Dunitz, J. D.; Seiler, P. *Acta Crystallogr. Ser. B* **1973**, *B29*, 589–595.
- (33) Koritsanzky, T.; Howard, S. T.; Mallinson, P. R.; Su, Z.; Richter, T.; Hansen, N. K. *XD—Computer Program Package for Multipole Refinement and Analysis of Electron Densities from Diffraction Data*, Version 1995.
- (34) Helminger, P.; De Lucia, F. C.; Gordy, W. *J. Mol. Spectrosc.* **1971**, *39*, 94.
- (35) Lide, D. R. *Handbook of Chemistry and Physics*, 72nd ed.; CRC: Boca Raton, FL, 1991.
- (36) Wiberg, K. B. *Acc. Chem. Res.* **1996**, *29*, 229–234.
- (37) Hirshfeld, F. L. *Israel J. Chem.* **1964**, *2*, 87–90.
- (38) Spackman, M. *Chem. Rev.* **1992**, *92*, 1769–1797.
- (39) Antipin, M. Yu.; Boese, R. Presented at the XVIIth Congress and General Assembly of the International Union of Crystallography, Seattle, WA, Aug. 8–17, 1996; Collected Abstracts, C418.
- (40) Antipin, M. Yu.; Timofeeva, T. V.; Yufit, D. S.; Sauer, J. *Russ. Chem. Bull.* **1995**, *44*, 2337–2345.